



Resonant x-ray emission spectroscopy at the L_3 edge of americium up to 23 GPa

S. Heathman,¹ J.-P. Rueff,^{2,3} L. Simonelli,⁴ M. A. Denecke,⁵ J.-C. Griveau,¹ R. Caciuffo,¹ and G. H. Lander¹

¹Joint Research Centre, Institute for Transuranium Elements, European Commission, Postfach 2340, D-76125 Karlsruhe, Germany

²Synchrotron SOLEIL, L'Orme des Merisiers, BP 48, Saint Aubin, 91192 Gif sur Yvette, France

³Laboratoire de Chimie Physique-Matière et Rayonnement, CNRS-UMR 7614, Université Pierre et Marie Curie, F-75005 Paris, France

⁴European Synchrotron Radiation Facility, BP 220, F-38043 Grenoble, France

⁵Institut für Nukleare Entsorgung, Karlsruhe Institut für Technologie (KIT), Postfach 3640, D-76021 Karlsruhe, Germany

(Received 11 October 2010; published 12 November 2010)

Resonant x-ray emission spectroscopy and x-ray absorption near-edge structure experiments have been performed on Am metal at the L_3 edge as a function of pressure. The hypothesis that the Am valence change at high pressure is associated with a mixing of the $5f^6$ and $5f^7$ configurations, hybridized with the $6d$ valence band, is not substantiated by the experiments. Neither the measured resonant x-ray emission spectroscopy nor x-ray absorption near-edge structure exhibit additional features expected for mixed valence. Only a small shift $\sim +2$ eV of the L_3 edge energy position and a decrease in white line intensity at high pressure is observed. The experimental results at higher pressure may be reproduced by increasing the $6d$ bandwidth and occupation and increasing the $5f$ bandwidth without any change in occupation. Further progress should be directed toward experiments at the Am M edges to observe directly the $5f$ states.

DOI: [10.1103/PhysRevB.82.201103](https://doi.org/10.1103/PhysRevB.82.201103)

PACS number(s): 71.28.+d, 71.30.+h, 75.30.Mb, 71.27.+a

Americium has a crucial place in the actinide series; it lies directly below Eu in the periodic table, has nominally six $5f$ electrons, and appears to be the first element in which the $5f$ electrons are localized.^{1,2} However, upon compression the structure of Am (double hexagonal close packed at ambient pressure) changes and goes through four phases between ambient and 17 GPa.³ In α uranium the $5f$ electrons are itinerant and the material exhibits a large bulk modulus, which is assumed to arise from the strong bonding (including contributions from the $5f$ electrons). At high-pressure Am adopts a similar structure to that of α uranium and has a similar large bulk modulus (more than double that at ambient pressure) so the analogy has been drawn that the $5f$ electrons in compressed Am are itinerant. Further support for a significant change in Am electronic structure as a function of pressure comes from measurements of the superconducting temperature.⁴ The interpretation in terms of delocalization (or Mott transition) is further supported by calculations.⁵⁻⁸ Although most⁵⁻⁷ of these calculations focus on structural aspects of the transitions in Am, the most recent⁸ discusses the mechanism in which the $5f$ states become delocalized. Using dynamical mean field theory calculations, an approach well suited to capture the interaction of f electrons with conduction states, these authors claim⁸ that the f^6 ground state of the atom starts to admix with a f^7 configuration. Because of hybridization with the spd bands, the large spin of the f^7 state ($J=7/2$) becomes screened (via the Kondo mechanism), and thus lowering the energy of the system. A surprising outcome of this statement is the prediction of a valence decrease in Am under pressure in opposition to the general trend in f -electron systems.

We set out to observe this electronic transition in Am experimentally by means of resonant x-ray emission spectroscopy (RXES) and x-ray absorption near-edge structure (XANES) both in conventional transition mode and in high resolution by measuring partial fluorescence yield (PFY-XANES; cf. below). The RXES technique has been used

extensively for lanthanide materials⁹ (and also for the high- T_c cuprates¹⁰) and has been successful in showing how the $4f$ configurations change with pressure. The resonant technique requires choice of an absorption edge; for the lanthanides all experiments so far have been done at the $L_{2,3}$ edges (5.7–9.0 keV). In our experiments we selected the Am L_3 edge (18.518 keV) since these photons can easily penetrate a pressure cell. Use of the $M_{4,5}$ edges, e.g., the M_4 edge at 4.092 keV (Ref. 11) would be difficult, although these resonances would probe $5f$ states more directly (a $3d \rightarrow 5f$ transition). The $L_{2,3}$ edges involve dipole allowed $2p \rightarrow d$ transitions and are primarily sensitive to changes in the (partially) occupied $6d$ valence band. Observation of the influence of the f states at these edges only occurs through their mixing with the valence band. Such observations have been successful for pressure experiments on Ce,¹² SmS,¹³ TmTe,¹⁴ Yb,¹⁵ and YbAl₃ (Ref. 16) with a mixed-valent signal observed in each case. By mixed valent we imply a configuration interaction that involves describing the ground-state wave function of the conduction $6d$ electrons as a superposition of $6d$ together with some fractional $5f$ character.

There is only one experiment of this type involving $5f$ systems; those reported in Ref. 17 on UPd₂Al₃ and UPd₃. In this work no sign of any $5f$ mixing into the $6d$ states was observed as a function of pressure. However, in contrast to the case of Am,⁵⁻⁸ current theories for these uranium systems do not suggest any change in this mixing as a function of pressure.

The sample was prepared at the Institute for transuranium elements. A piece of americium metal (²⁴³Am isotope) was thermally annealed and characterized by superconducting quantum-interference device measurements. Thin foils < 5 μm thick were then prepared by rolling and a small piece cut and loaded into a 130 μm hole of an inconel gasket along with a couple of small < 8 μm diameter ruby spheres for pressure measurement.

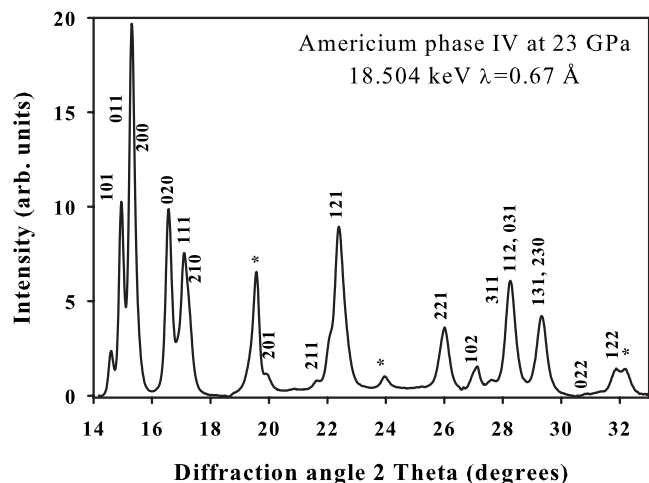


FIG. 1. Diffraction pattern recorded at ID16 of orthorhombic (space group $Pnma$) Am phase IV at 23 GPa showing principal reflections. Peaks due to the gasket are marked with an asterisk (*).

A specially designed wide aperture membrane-type diamond-anvil cell (MDAC) incorporating thin 1.5-mm-high diamonds was used to contain the americium sample. Silicone oil was used as the pressure-transmitting medium. This design reduces the absorption of the sample signal by the diamond anvils and also the Compton scattering originating from the diamonds.

A standard LaB_6 sample loaded into an identical MDAC was used to calibrate the instrument parameters. The smallest practical x-ray beam dimension we were able to obtain at 18.504 keV on the ID16 beamline at the European Synchrotron Radiation Facility (ESRF) for powder diffraction was $20 \times 130 \mu\text{m}$. Before each spectroscopy measurement, the ruby luminescence wavelength inside the MDAC was measured to determine the pressure and an Am diffraction pattern registered at 18.504 keV using a MAR-165 charge coupled device detector. The diffraction images were processed using the ESRF FIT2D program to produce integrated profiles. The pattern obtained for the Am IV phase at 23 GPa is shown in Fig. 1; it is comparable to that reported earlier.³

Conventional Am L_3 XANES of Am in the MDAC as a function of pressure up to 20 GPa were measured at the INE-Beamline for actinide research¹⁸ at the ANKA synchrotron. The energy position at the XANES white line (WL) intensity maximum (E_{max}) was observed to shift about +1.0 eV between ambient pressure and 20 GPa, and the WL intensity decreased significantly. None of the spectra exhibited a pre-edge feature. The XANES WL contains information concerning unoccupied $6d$ states. XANES fits of the spectra reveal the WL intensity decrease at high pressure involves a decrease in both height and area, suggesting a higher $6d$ -like state population. The WL full width at half maximum was determined from the fits to be 14 eV at ambient pressure and 12 eV at 20 GPa.

RXES experiments were done on ID16 at the ESRF (Ref. 19) by monitoring the energy dependence of the Am $L\alpha_1$ emission line at $E_2 = 14.625$ keV, corresponding to $3d_{5/2} \rightarrow 2p_{3/2}$ emission after the initial process of creating a $2p_{3/2} \rightarrow 6d_{5/2}$ core hole by photons tuned around the L_3 ion-

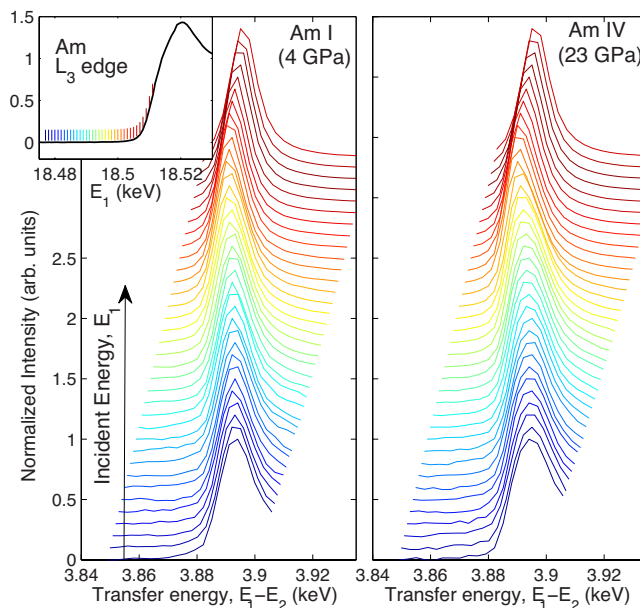


FIG. 2. (Color online) Resonant emission x-ray scattering intensity for Am phase I at 4 GPa and phase IV at 23 GPa as a function of transfer energy (difference between incident and emission energies) measured at various incident photon energies (E_1), increasing from bottom to top. For clarity, the spectra have been normalized to the same maximum intensity and vertically offset.

ization energy (E_0). The advantage, as explained in Ref. 17, is that the energy resolution is intrinsically improved, as it is not determined by the short $2p_{3/2}$ core-hole lifetime (7.4 eV) (Ref. 20). In the PFY-XANES measurements, the final energy (E_2) was kept fixed at the $L\alpha_1$ energy and the incident energy (E_1) tuned through the L_3 edge (E_0). Inversely for RXES, the final energy was varied at fixed incident energy. The RXES spectra reflect final-state energy distributions in the presence of a $3d$ core hole and are especially sensitive to mixed-valent character. Measurements were repeated for a series of pressures up to 23 GPa, i.e., into the Am IV phase. At the end of the series, the pressure was released and spectra again recorded.

Figure 2 shows the experimental RXES data recorded at 4 and 23 GPa. The width of these spectra is about 11 eV, which is considerably larger than those for lanthanides, which are about 50% narrower (see, e.g., Refs. 9 and 12). The U $3d$ core hole, which contributes to the width of the $L\alpha_1$ emission line, is about 3.3 eV (Ref. 21) and the instrumental resolution at $E_2 \sim 14$ keV is approximately 4 eV (compared to ~ 2 eV in the case of Ce emission⁹), so we should expect a final width of around 7 eV, which is less than the measured 11 eV. The contribution from the $6d$ bandwidth to the spectral width must also be considered. The $6d$ bandwidth is considerably broader than the equivalent $5d$ valence band in the lanthanides. Clearly, the $6d$ bandwidth limits the resolution here. Similar broad spectra were observed in the case of UPd_2Al_3 and UPd_3 .¹⁷

The integrated PFY-XANES are plotted as a function of E_1 in Fig. 3. As observed in the conventional Am L_3 XANES, these spectra show clearly a decrease in WL intensity and shift in E_{max} to higher energy as a function of pres-

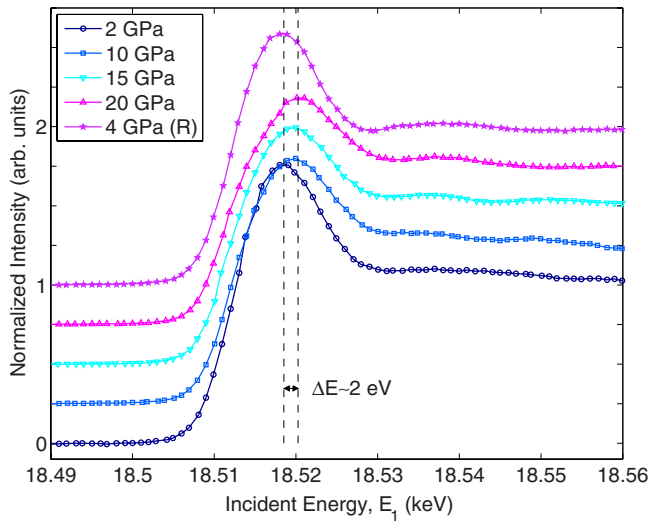


FIG. 3. (Color online) The PFY-XANES from integrated $L\alpha_1$ intensities recorded across the Am L_3 edge. The overall shift between low and high pressures is $+2.0(3)$ eV.

sure. There is a concurrent shift in the first inflection point toward lower energy. The shift in E_{\max} from ambient to 23 GPa is $+2.0(3)$ eV and $-1.5(5)$ eV in the inflection point. A similar shift is reported for UPd_2Al_3 (Ref. 17) at its phase transition at 23 GPa and also for USb under pressure.²² In analogy with the discussion of UPd_2Al_3 ,¹⁷ this could be interpreted as an increase in valence, perhaps with a change in Am ground state from $5f^6$ to $5f^{6-\delta}$. However, there are many caveats to this conclusion; the transition with pressure in Am between ambient pressure and 20 GPa involves a 40% volume reduction and a change in the bulk modulus from 30 to

100 GPa. In the case of UPd_2Al_3 (and USb) the decrease in volume and change in the bulk modulus as a function of pressure are much smaller.

Disappointingly, there is no sign of any mixed-valent character in either Fig. 2 and 3, which would appear as an additional signal associated with mixing of $5f$ states such as those observed for the lanthanides.^{9,12-16} If, as suggested by Savrasov *et al.*,⁸ the $5f^7$ state starts to mix with the valence band a spectral feature should have appeared on the left-hand side (lower energy) of the peak in Fig. 2 and the WL in Fig. 3. This, for example, is the case for SmS,¹³ where the lower valence state (Sm^{2+} with one additional f electron) mixes with the valence band and exhibits an additional emission about 13 eV below the normal-emission peak. No analogous peak is observed for Am. Am also does not show any additional emission intensity on the right-hand side (higher energy) of the normal-emission peak, as is observed for the lower f -count state in TmTe (Ref. 14) with the two $4f$ configurations separated by ~ 7 eV. Although our resolution is noticeably worse than that available for RXES in the lanthanides (as we have discussed this is likely intrinsic,¹⁷ arising from the larger $6d$ bandwidth compared to that of the $5d$ states in the lanthanides), we believe it is sufficient to detect any mixing of the $5f$ states of Am at high pressure, if such effects existed.

In order to understand the spectral changes in the XANES, the spectra and electronic structures were calculated using the self-consistent, real-space multiple-scattering method implemented in the *ab initio* FEFF code (version 9.0) (Ref. 23) for simple Am clusters (cf. insets in Fig. 4) having Cartesian coordinates of the ambient-pressure phase [phase I, ICSD 609752], of the phase III at 15 GPa and of the high-pressure phase [phase IV, ICSD 43805]. Calculations are performed using default exchange-correlation potentials, full-

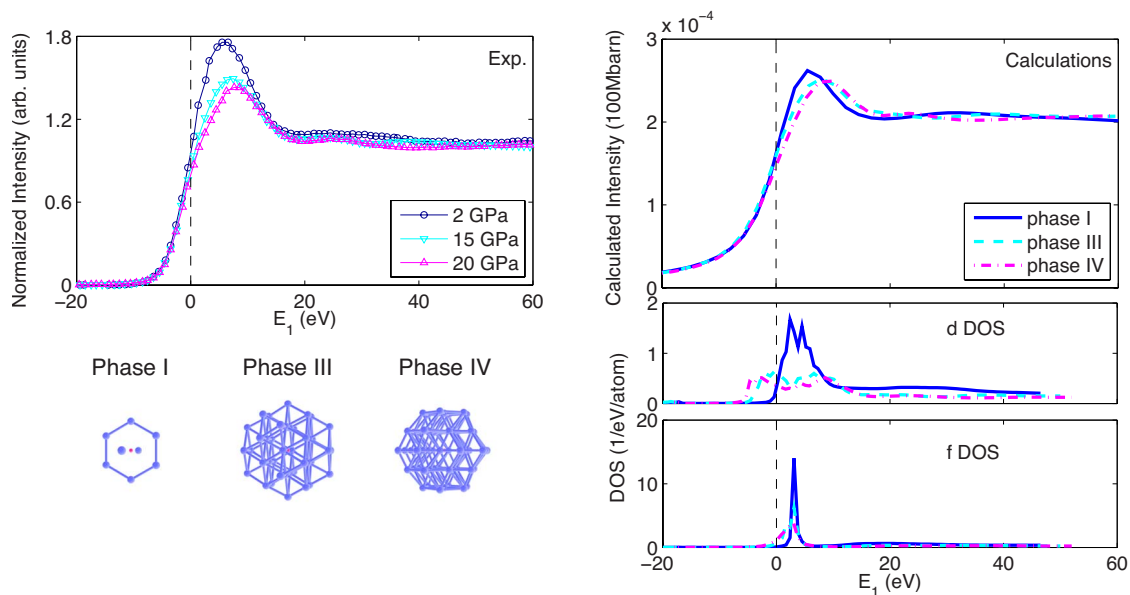


FIG. 4. (Color online) Experimental Am L_3 PFY-XANES recorded for Am at the pressures indicated (left) and theoretically calculated spectra and projected local density of d and f states for the Am phases I, III, and IV. The incident-energy scale is referred to the Fermi energy taken at the inflection point (dashed line). The clusters used for the calculations are shown in the lower left part; the absorbing site is on the central atom. See text for details.

multiple scattering, and nonscreened core hole. The resulting theoretical XANES and the projected local density of states (*l*-DOS; *d* and *f* states) for the central absorbing Am are depicted in Fig. 4, right; for comparison, the experimental spectra are shown at left. The theoretically calculated XANES are in good qualitative agreement with experiment. Especially, the postedge features around 20 eV and their change at high pressure are well reproduced, indicating that these are mostly of *d* character. Note however that both *f*-*d* bands are strongly hybridized in this energy region. The decrease in WL intensity and increase in E_{\max} in the high-pressure phase compared to the ambient-pressure phase are both reproduced. The calculations indicate a significant broadening of the *d*-DOS at higher pressure, as well as an increase in electron count for this orbital momentum to 2.0 (from 0.8 in the Am phase I). Qualitatively, this would explain the WL intensity decrease: lower state density and higher state occupancy with associated decrease in photoelectron transition probability. Similarly, the opposite shift of the WL energy and of the inflection point are well accounted for by the redistribution of spectral weight in the *d* band. The calculations also indicate a broadening of the *5f* DOS upon

increasing pressure (but no change in electron count). Finally the overall agreement with calculations performed in a band approach exclude strong multielectronic effects in the Am L_3 edge. It also indicates the limitations of the L_3 edge as a probe of the *f*-electron valence in Am.

In conclusion, our experiments show that there is no evidence for any mixed-valent character at the L_3 edge spectra in the high-pressure Am phase IV. They have not, however, resolved the exact nature of the valence transition in Am metal as a function of pressure. Proposed models suggesting a strong mixing of *5f* states with the valence band in the high-pressure phase, as occurs frequently in the mixed-valence lanthanide systems,⁹ are not consistent with our experimental results. To resolve this puzzle, further progress should be directed toward experiments at the Am $M_{4,5}$ edges to observe directly the *5f* states.

We thank D. Bouëxière and R. Eloirdi of ITU for the preparation of the ²⁴³Am foil, and Patrick Colomp of the radioprotection group of the ESRF for his help during the experiment. We have benefited from discussions with Gabi Kotliar, to whom we express our thanks.

-
- ¹G. H. Lander, *Science* **301**, 1057 (2003).
²K. T. Moore and G. van der Laan, *Rev. Mod. Phys.* **81**, 235 (2009).
³S. Heathman, R. G. Haire, T. Le Bihan, A. Lindbaum, K. Litfin, Y. Méresse, and H. Libotte, *Phys. Rev. Lett.* **85**, 2961 (2000).
⁴J.-C. Griveau, J. Rebizant, G. H. Lander, and G. Kotliar, *Phys. Rev. Lett.* **94**, 097002 (2005).
⁵P. Söderlind, R. Ahuja, O. Eriksson, B. Johansson, and J. M. Wills, *Phys. Rev. B* **61**, 8119 (2000).
⁶M. Pénicaud, *J. Phys.: Condens. Matter* **17**, 257 (2005).
⁷P. Söderlind and A. Landa, *Phys. Rev. B* **72**, 024109 (2005).
⁸S. Y. Savrasov, K. Haule, and G. Kotliar, *Phys. Rev. Lett.* **96**, 036404 (2006).
⁹J.-P. Rueff and A. Shukla, *Rev. Mod. Phys.* **82**, 847 (2010).
¹⁰L. Braicovich *et al.*, *Phys. Rev. Lett.* **102**, 167401 (2009).
¹¹D. Mannix, S. Langridge, G. H. Lander, J. Rebizant, M. J. Longfield, W. G. Stirling, W. J. Nuttall, S. Coburn, S. Wasserman, and L. Soderholm, *Physica B* **262**, 125 (1999).
¹²J.-P. Rueff, J.-P. Itié, M. Taguchi, C. F. Hague, J.-M. Mariot, R. Delaunay, J.-P. Kappler, and N. Jaouen, *Phys. Rev. Lett.* **96**, 237403 (2006).
¹³E. Anese, A. Barla, C. Dallera, G. Lapertot, J.-P. Sanchez, and G. Vankó, *Phys. Rev. B* **73**, 140409(R) (2006).
¹⁴I. Jarrige, J.-P. Rueff, S. R. Shieh, M. Taguchi, Y. Ohishi, T. Matsumura, C.-P. Wang, H. Ishii, N. Hiraoka, and Y. Q. Cai, *Phys. Rev. Lett.* **101**, 127401 (2008).
¹⁵C. Dallera *et al.*, *Phys. Rev. B* **74**, 081101(R) (2006).
¹⁶R. S. Kumar, A. Svane, G. Vaitheeswaran, V. Kanchana, E. D. Bauer, M. Hu, M. F. Nicol, and A. L. Cornelius, *Phys. Rev. B* **78**, 075117 (2008).
¹⁷J.-P. Rueff, S. Raymond, A. Yaresko, D. Braithwaite, P. Leininger, G. Vankó, A. Huxley, J. Rebizant, and N. Sato, *Phys. Rev. B* **76**, 085113 (2007).
¹⁸M. A. Denecke, J. Rothe, K. Dardenne, H. Blank, and J. Hormes, *Phys. Scr.* **T115**, 1001 (2005).
¹⁹R. Verbeni, T. Pylkkänen, S. Huotari, L. Simonelli, G. Vankó, K. Martel, C. Henriquet, and G. Monaco, *J. Synchrotron Radiat.* **16**, 469 (2009).
²⁰M. O. Krause and J. H. Oliver, *J. Phys. Chem. Ref. Data* **8**, 329 (1979).
²¹D. A. Zatsepin, S. M. Butorin, D. C. Mancini, Y. Ma, K. E. Miyano, D. K. Shuh, and J. Nordgren, *J. Phys.: Condens. Matter* **14**, 2541 (2002).
²²S. Yagoubi, S. Heathman, M. Denecke, J. Römer, and G. H. Lander, ANKA Annual Report, 2008, p. 153, http://ankaweb.fzk.de/_cms/_release/extras/downloads.php
²³A. L. Ankudinov, B. Ravel, J. J. Rehr, and S. D. Conradson, *Phys. Rev. B* **58**, 7565 (1998).